Case Studies in Engineering Failure Analysis 2 (2014) 15–24

Contents lists available at ScienceDirect

Case Studies in Engineering Failure Analysis

journal homepage: www.elsevier.com/locate/csefa

Short communication

Investigation on brittle fracture mechanism of a grade E cast steel knuckle

Jin Huang *, Lu Xia, Youshou Zhang, Sinian Li

Hubei Provincial Key Laboratory of Green Materials for Light Industry, Hubei University of Technology, Wuhan 430068, PR China

ARTICLE INFO

Article history:
Received 13 May 2013
Received in revised form 15 November 2013
Accepted 5 December 2013
Available online 5 January 2014

Keywords:
Knuckle
Grade E cast steel
Dendrites
Shrinkage porosity
Brittle fracture

ABSTRACT

This paper investigated the brittle fracture mechanism of a grade E cast steel knuckle that is one of the key components of the coupler for railway wagon by using scanning electronic microscope, optical microscope, energy dispersive spectroscopy as well as mechanical property testing methods. It is found that large amounts of developed coarse dendrites and shrinkage porosity existed in the knuckle's microstructure, the plasticity and impact toughness of the knuckle entity are very bad and far below that of the Keel block represented this knuckle. Apparently, the shrinkage porosity resulted in the knuckle unsound metallic matrix and poor mechanical properties. The fracture morphology mainly shows the characteristic of cleavage, quasi-cleavage fracture as well as a little ductile fracture, so the failure of the knuckle can be attributed to brittle fracture distinctly. Moreover, a welding repair area with high hardness is also found in the fracture region, which might initiate micro-cracks on the surface of the knuckle. As a result, it can be inferred that under an impact load that did not exceed material fracture limit, the micro-cracks initiated from weld repair zone propagated rapidly into the inner matrix by continuously fracturing the dendrites along shrinkage porosity regions until the knuckle failed instantly.

1. Introduction

The knuckle is one of the key components of coupler assembled in the railway wagon. It is mainly exposed to traction, compression brought about by the alternating load. Once the knuckle broke a vehicle separation accident will happen, so it is essential for its safety and reliability. Currently, the knuckle is based on the casting manufacturing with grade E cast steel in accordance with the specification of AAR-M201 (one of standards for American Association of Railroads). The grade E cast steel possesses the features of high tensile strength and high yield strength/tensile strength ratio [1]. However, in the last decade years, with the railway freight cars running speed, traction tonnage increasing, railway vehicles with cast knuckle fracture accident is gradually increasing, which seriously threaten to railway transportation safety. Based on previous investigation on knuckle fracture mechanism, the failure of knuckles may be ascribed to some reasons. One is the irrational design resulting in high stress concentration or fatigue cracking at the local regions of a knuckle [2–4]. The second can be the casting defects decreasing mechanical properties, such as mis-run, cold lap, hot crack and non-metallic inclusions [5,6]. The third is the corrosion inducing initiation of micro-crack on a knuckle surface

* Corresponding author. Tel.: +86 13871199385.
E-mail addresses: huangjin215@126.com (J. Huang), xl9195@126.com (L. Xia), youshou3114@sina.com (Y. Zhang), lisn@mail.hbut.edu.cn (S. Li).

2213-2902
http://dx.doi.org/10.1016/j.csefa.2013.12.007

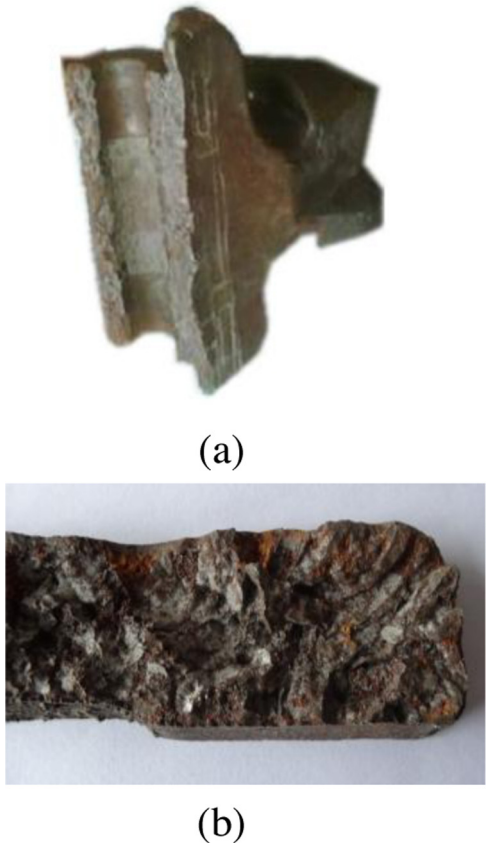

Fig. 1. Photographs of failed knuckle (a); the fracture surface of the knuckle (b).

[7] and the incorrect heat-treatment practices producing low plasticity and toughness, which results in nucleation and propagation of crack [8]. The poor welding repair can also result in material high hardness and poor toughness as well as surface micro-crack [9]. And improper vehicle operation can bring about a huge instant impact load that could exceed strength limit of the cast steel [10].

In the present work, we investigated the brittle fracture of a knuckle made of grade E cast steel and found that the failure cause of the knuckle were different from that of those mentioned above, which may ascribe to its special solidification microstructure feature of the cast steel.

2. Making and failure

The failed knuckle used in present investigation, as shown in Fig. 1a, came from a railway wagon that was used to transport iron ore in an iron mine in Australia. The fracture of this knuckle occurred at the fifteenth day of its service. Its fracture view is demonstrated in Fig. 1b and appears a characteristic of brittle fracture. This knuckle was cast in green sand mold with grade E cast steel. During heat treatment process, it was firstly normalized at 900–920 °C for 3.5–4 h and cooled in the air, then heated up to 870–880 °C and holding time was 3–3.5 h, quenched in water, and finally followed by tempering of 510–550 °C for 3.5–4 h and cooled in water again. The microstructure of the knuckle after heat treatment is tempered sorbite. Tables 1 and 2 summed the chemical compositions and mechanical properties of Keel block of the knuckle and corresponding to the standard values of AAR-M201 grade E cast steel. It can be seen that

Table 1
Chemical compositions of Keel block and AAR-201 grade E cast steel (wt.%).

	C	Si	Mn	P	S	Cu	Cr	Ni	Mo	Al	Fe
AAR-M201 grade E cast steel	≤0.32	≤1.50	≤1.85	≤0.040	≤0.040						Balance
Keel block	0.23	0.34	1.40	0.025	0.026	0.110	0.46	0.96	0.21		Balance

Table 2
Mechanical properties of Keel block and AAR-201 grade E cast steel.

	$R_{PO.2}$ (MPa)	Rm (MPa)	Elong (%)	R of A (%)	A_{KV} (J, −40 °C)			
					1	2	3	Average
AAR-M201 grade E cast steel	690	827	14	30	1			27
Keel block	935	995	16.0	42.5	51	49	37	46

the chemical compositions and mechanical properties of the Keel block fit the standard requirement of AAR-M201 grade E cast steel.

3. Experimental

3.1. Specimen preparation

The samples used in the present work were cut from the failed knuckle as shown in Fig. 1a. The sampling method can be described as follows: Firstly, two plate-shape blocks labeled as 1# and 2# respectively were cut from the region adjacent to the fracture surface of the knuckle by sawing method, as shown in Fig. 2; Secondly, the specimens for tensile testing and Charpy impact testing were cut from the plate-shape block 1#, respectively, as shown in Fig. 3a. The specimens labeled as A, B, C, D, E, F and G were cut from the plate-shape block 2#, respectively, as shown in Fig. 3b. The specimens B, C, D, E, F and G were used for fracture morphology observation and the specimens A and E were used for solidification microstructure analysis, respectively. The specimens for chemical composition analysis and metallographic observation came from the tested Charpy impact specimens. After the plate-shape blocks were cut off, a weld area with high hardness on the sectioned surface of the failed knuckle is clearly discernible, as shown in Fig. 4. Specimens for metallographic and solidification microstructure observation were grinded, polished, and then etched with 3% nital and nitroxanthic acid.

3.2. Experimental methods

Chemical composition analysis was conducted using spectral detector (SPECTROMAXx, Germany). Tensile testing and Charpy impact toughness testing were performed using microcomputer controlled electro-hydraulic servo universal testing machine (SHT5605) and impact testing machine, respectively. Microstructure and fracture morphology were observed using optical microscope (OM, OLYMPUS, GX51, Japan) and scanning electronic microscope (SEM, JEOJSM-6390LV, Japan), respectively. Impurity elements analysis was carried out employing energy dispersive spectroscopy (EDS, 7582X, OXFORD, Britain).

4. Results and discussions

4.1. Chemical composition and mechanical properties

The chemical composition and the mechanical properties adjacent to the fracture region of the failed knuckle are listed in Tables 3 and 4, respectively. As shown in Table 3, the chemical composition of the knuckle satisfies the standard requirement according to AAR-M201. However, the level of aluminum reaches up to a high level of 0.088%. Excessive aluminum in steel may form aluminum nitride (AlN) hardening phase at grain boundaries, which can result in the brittle fracture of steel [11]. From Tables 2 and 4, it can be found that the mechanical properties of the failed knuckle entity are far below that of the Keel

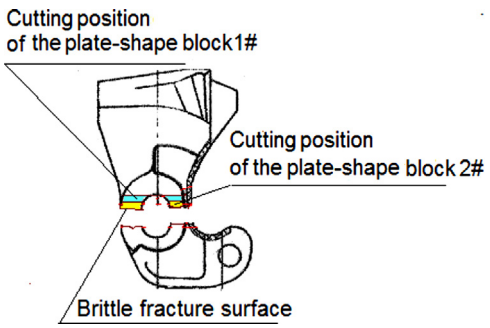

Fig. 2. Schematic diagram of cutting positions of two plate-shape blocks on the failed knuckle.

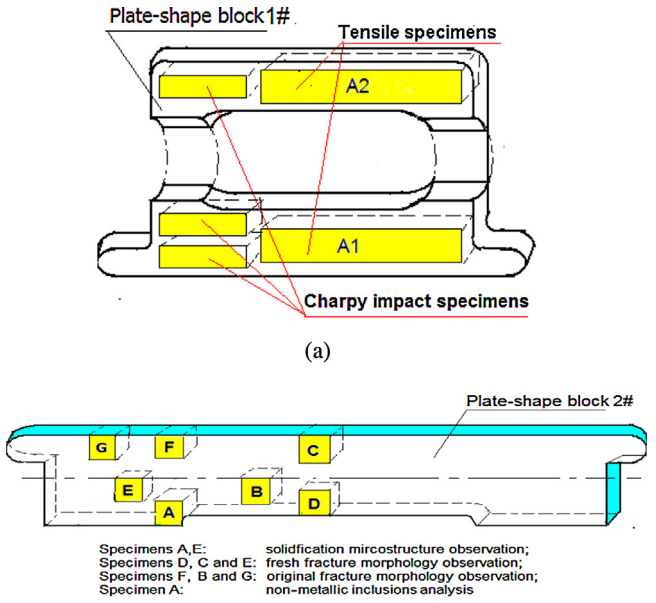

Fig. 3. Schematic diagram of sampling positions of specimens of the knuckle; for tensile and Charpy impact testing (a); for microstructure and fracture morphology observations (b).

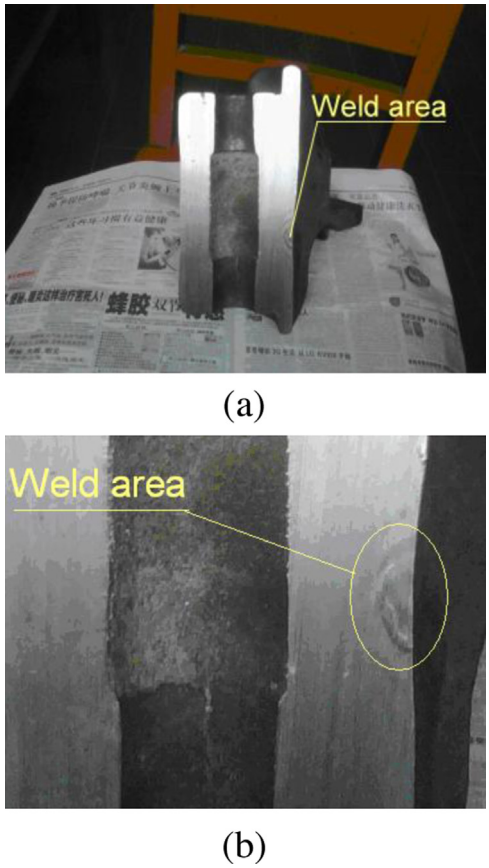

Fig. 4. A weld area located on the sectioned surface of the failed knuckle (a); an enlarge view of the weld area (b).

Table 3
Chemical composition of the failed knuckle entity (wt%).

	C	Si	Mn	P	S	Cu	Cr	Ni	Mo	Al	Fe
Analyzing values of entity	0.27	0.28	1.48	0.023	0.018	0.113	0.480	0.99	0.212	0.088	Balance

Table 4
Mechanical properties of the failed knuckle entity.

	$R_{PO.2}$ (MPa)	Rm (MPa)	Elong (%)	R of A (%)	A_{KV} (J, −40 °C)			
					1	2	3	Average
Testing values of entity (A1)	–	920	5.5	26	11	11	10	10.7
Testing values of entity (A2)	–	845	3.0	5.5	–	–	–	–

block and do not satisfy AAR-M201 standard. The elongation and Charpy impact toughness values only are 3.0–8.5% and 10.7–18.5 J, respectively. Even its yield strength could not be measured out. The results tested demonstrate that the material of the failed knuckle entity possesses the brittlement feature and the mechanical properties of the Keel block cannot represent the mechanics performance of the failed knuckle entity.

4.2. Metallographic observation

Fig. 5 is the metallographic photos adjacent to the fracture surface of the failed knuckle. It can be seen that the microstructure of the knuckle mainly consists of tempered sorbite. However, the undissolved ferrite phase (the white areas in the metallographic photos) and coarse crystal grains are also found in these photos. This means that the knuckle's metallic matrix was not austenitized completely before quenching during heat treatment, which also resulted in the poor mechanical properties.

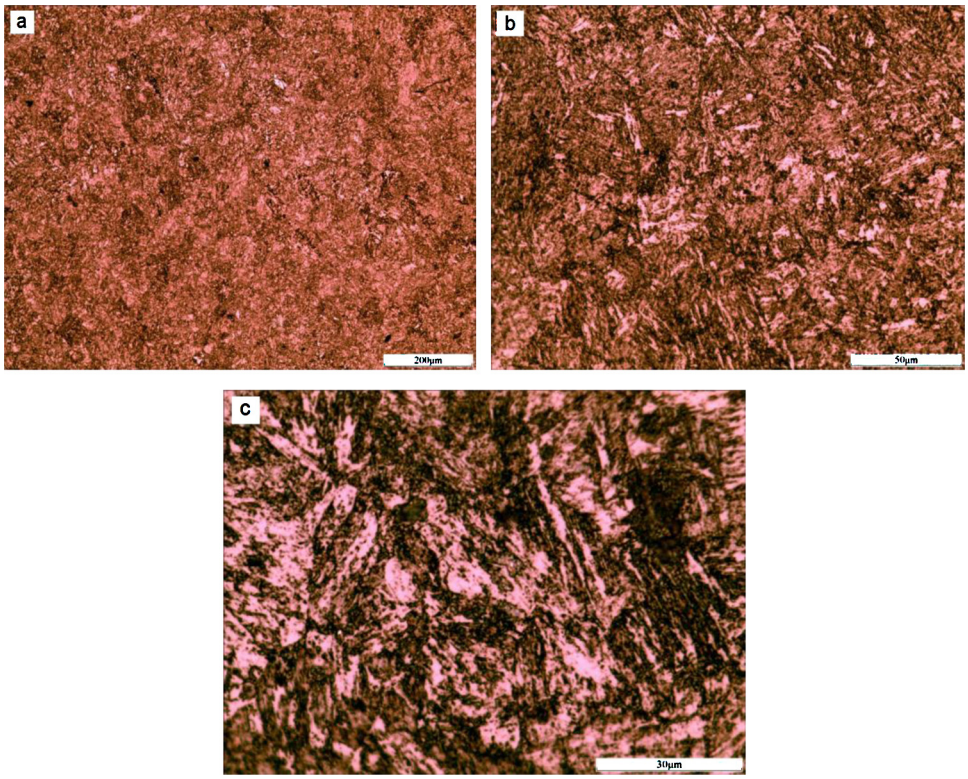

Fig. 5. Metallographic photos of the failed knuckle entity, (a) 100×, (b) 500×, (c) 1000×.

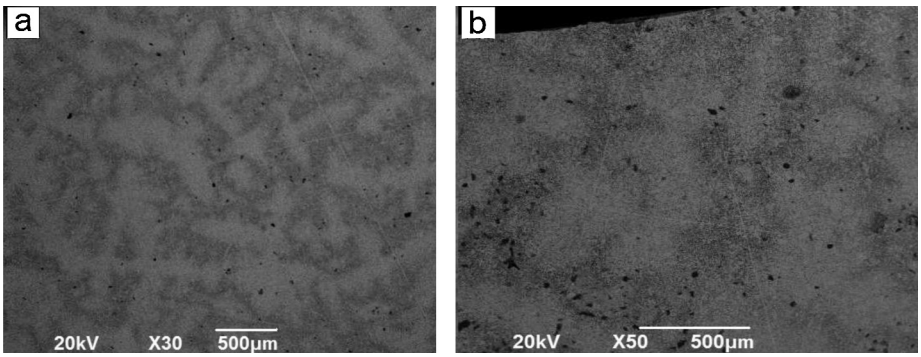

Fig. 6. SEM images of solidification microstructure adjacent to the fracture surface of the failed knuckle: (a) specimen A; (b) specimen E.

4.3. Microstructure characteristic

Fig. 6 is the SEM images of the solidification microstructure in the specimens A and E. It can be clearly identified that the solidification microstructure of the failed knuckle primarily consists of developed coarse dendrites (light gray areas in Fig. 6a–b). The diameter and length of their primary dendrite can reach 0.3 mm and 1 mm, respectively. Furthermore, large amounts of shrinkage porosity in interdendritic regions can be observed (dark gray and black spot areas in Fig. 6a–b), which have separated the metallic matrix and resulted in a decreasing in the mechanical properties.

4.4. Morphology of fresh fracture surface

In order to avoid the misjudgment caused by interference of fracture surface pollution, firstly, the fresh fracture surface of the failed knuckle was used in present investigation. The preparation method of fresh fracture surface is described as follows: a shallow notch (depth $\leq$1 mm) was transversely machined at center dot of the axial line on the surface of a specimen with size of 8 mm $\times$ 6 mm $\times$ 20 mm; then this specimen was fractured along the notch by hammering. Thus a fresh fracture surface on the specimen was created, as illustrated in Fig. 7.

Figs. 8–10 are SEM images of the fresh fracture morphology of specimens D, C and E, respectively. From the SEM images, it can be found that the solidification microstructure of the failed knuckle mainly consists of developed dendrites. Fig. 8b is a local enlarged view in Fig. 8a (indicated by arrow), where the dendrites look like grape clusters and there are large amounts of shrinkage porosity in interdendritic regions. The specimens were fractured along the free surfaces of the dendrites and gaps between dendrites. Fig. 9b and c are the SEM images of two local enlarged views of the fracture surfaces of dendrites in Fig. 9a (indicated by arrows 1 and 2, respectively), in where the tearing ridges, dimples and micro-void structures with ductile fracture features can be observed. Obviously, the fracture of the dendrites in the metallic matrix belongs to ductile fracture.

4.5. Morphology of original fracture surface

The original fracture surface is the failed knuckle's fracture surface formed in wagons running accident. Figs. 11–13 are the SEM images of original fracture surfaces of the specimens F, B and G. Fig. 11a shows the fracture appearance with cleavage and quasi-cleavage facet features, which can be ascribed to brittle fracture. Fig. 11b, a local enlarged view in Fig. 11a (indicated by arrow1), clearly displays trans-granular and inter-granular fracture surfaces. However, Fig. 12a demonstrates the dendritic structure feature. Fig. 12b is a local enlarged image in Fig. 12a. It reveals that the part microstructure of the

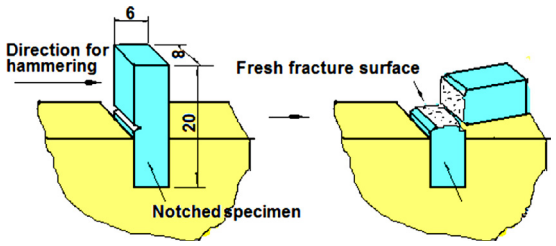

Fig. 7. Schematic diagram of fresh fracture surface preparation on the specimens.

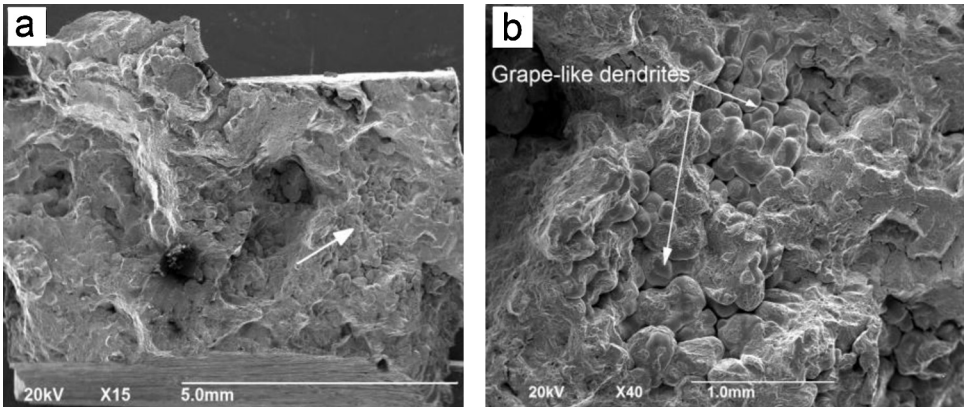

Fig. 8. SEM images of the fresh fracture surfaces of specimen D (a); a local enlarged view at a region indicated by arrow in (a), (b).

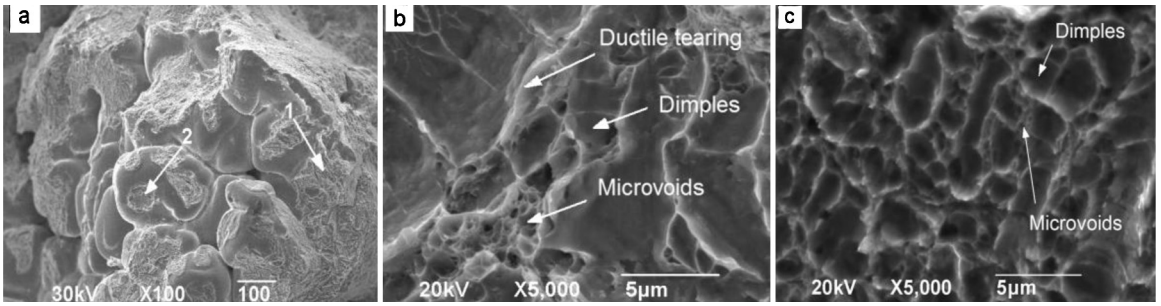

Fig. 9. SEM image of the fresh fracture surface of specimen C (a); the local enlarged views of the fracture surfaces of the dendrites at the regions indicated by arrows 1 and 2 in (a), (b) and (c), respectively.

metallic matrix consists of developed coarse dendrites with grape clusters shape and shrinkage porosities. Fig. 13 exhibits the quasi-cleavage fracture surfaces with less "river" and tearing ridge patterns. As a result, it can be identified that failure of the knuckle can be ascribed to the mixed type fracture with the features of cleavage and quasi-cleavage of brittle fracture and less ductile fracture.

4.6. Non-metallic inclusions

It is well known that large amounts of non-metallic inclusions or harmful elements such as sulphur, phosphorus, etc. distributed in the grain boundaries of steels will sharply decrease their fracture resistance behavior. As shown in Table 3, the mean levels of sulphur and phosphorus contained in the failed knuckle entity are 0.023 wt%

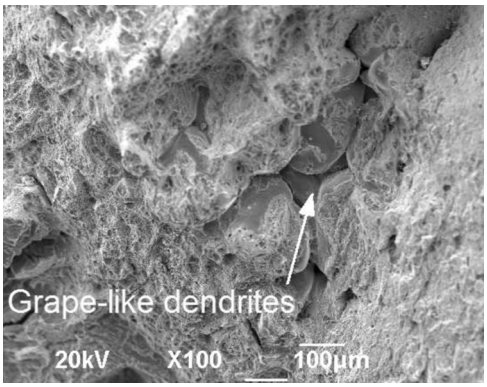

Fig. 10. SEM image of the fresh fracture surface of specimen E.

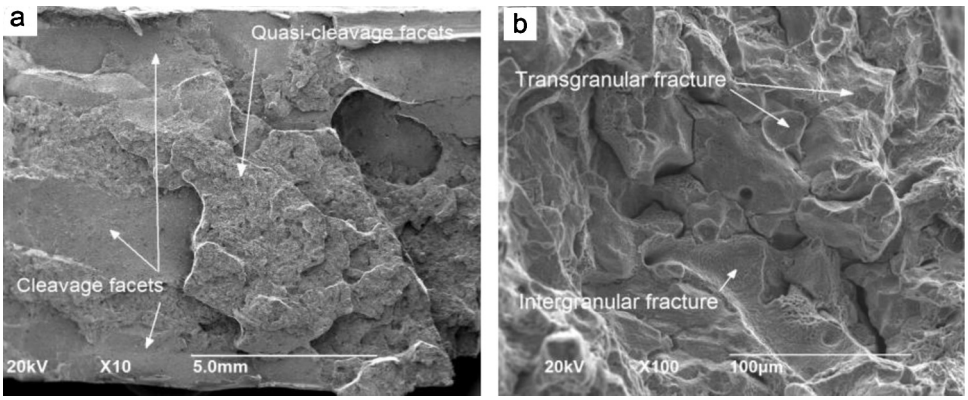

Fig. 11. SEM image of original fracture surface of specimen F (a); a local enlarged view in (a), (b).

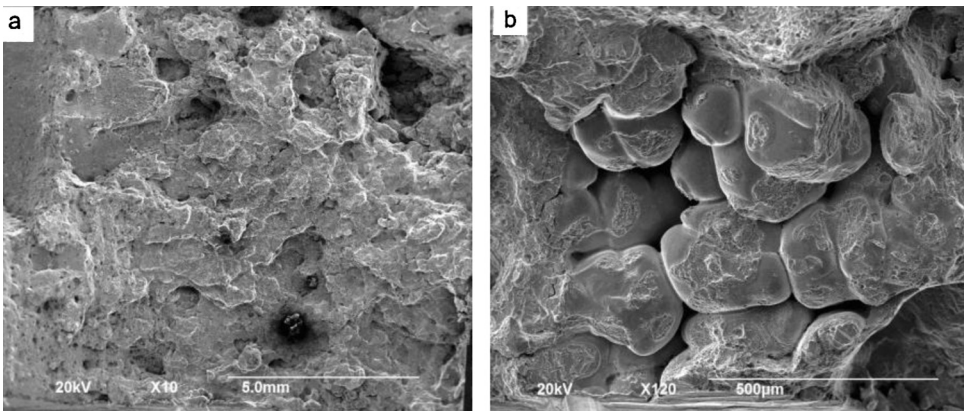

Fig. 12. SEM image of original fracture surface of specimen B (a); a local enlarged view in (a), (b).

and 0.018 wt%, respectively, which would not affect the knuckle's mechanical properties. But the level of aluminum reaches up to 0.088 wt%, which may lead to the formation of AlN hardness phase. Therefore, it is important to detect non-metallic inclusions or harmful elements in the fracture region of the failed knuckle. Fig. 14 shows the SEM image of specimen A with the detecting spots for EDS and the EDS spectra corresponding to each detecting spot (indicated by labels). In this image, the developed coarse dendrites (black-gray regions) as well as shrinkage porosity (gray-white regions and black spots) are clearly observed. The EDS spectra reveals that sulphur, phosphorus and aluminum as well as oxygen elements existed in interdendritic regions, whereas nothing of these elements is observed in the interior of dendrites. Therefore, a reasonable speculation is that the non-metallic inclusions such as manganese sulfide, silicate, alumina, phosphide existed in the interdendritic regions. Obviously, due to the existence of shrinkage porosity, fracture resistance behavior of the knuckle would be less affected by these non-metallic inclusions.

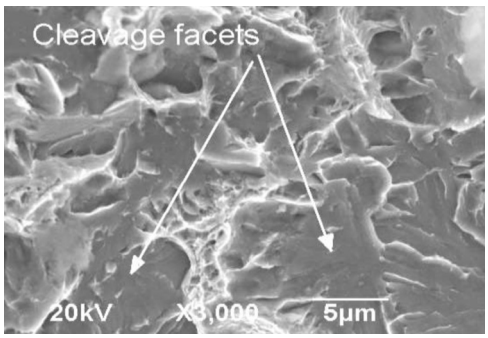

Fig. 13. SEM image of original fracture surface of specimen G.

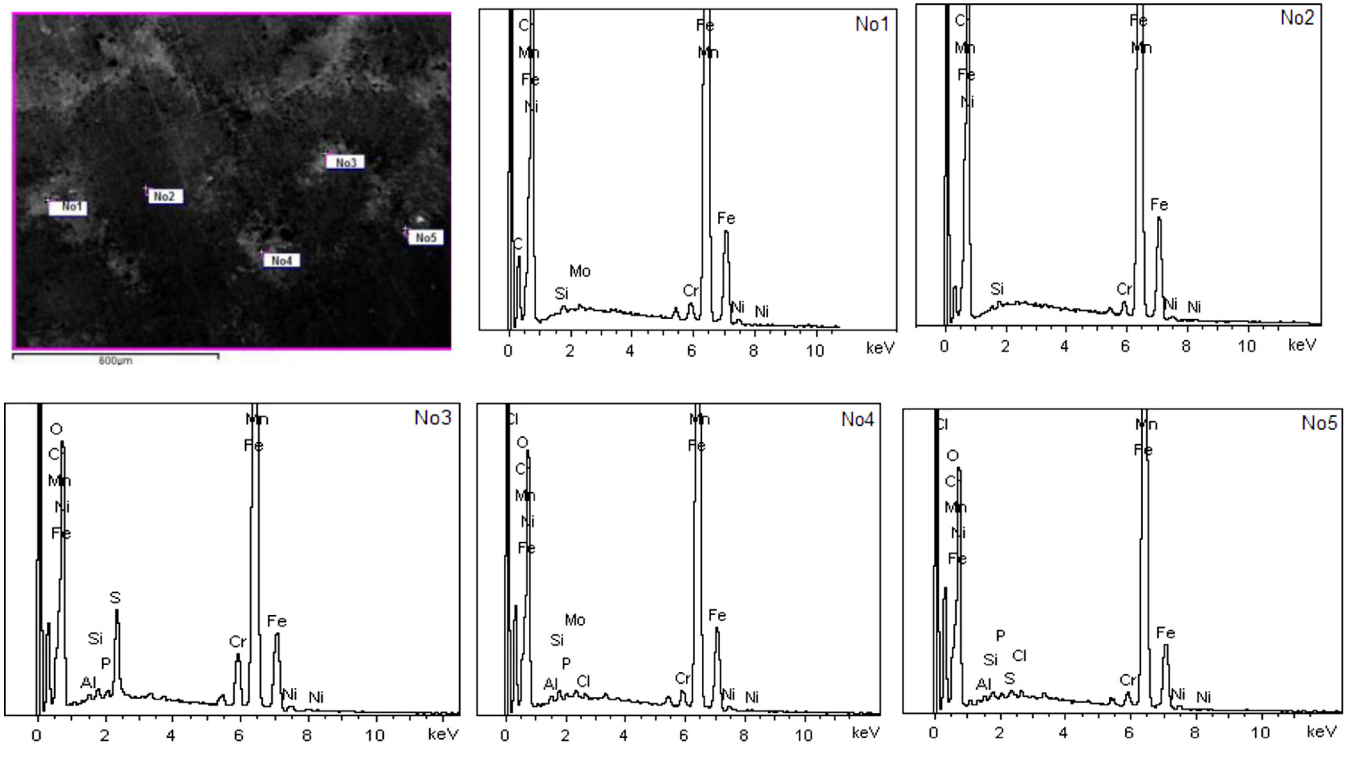

Fig. 14. SEM image of specimen A with detecting spots of EDS and EDS spectra corresponding to detecting spots (indicated by labels).

5. Summary and conclusions

5.1. Through this investigation, we can get the conclusions as follows

The mechanical properties of the Keel block of the failed knuckle fit the standard of AAR-M201 grade E cast steel, but the failed knuckle entity does not. The plasticity and impact toughness of the failed knuckle entity are far below that of the Keel block, and even its yield strength cannot be measured out, which indicates that the Keel block in mechanics performance cannot represent the knuckle entity, although both of them was cast in same sand mold and using the same liquid steel.

The solidification microstructure of the failed knuckle consists of developed coarse dendrites and large amounts of shrinkage porosity in inter-dendritic regions, which demonstrates that the metallic matrix of the failed knuckle entity is unsound. The fracture morphology mainly shows the characteristic of cleavage, quasi-cleavage fracture as well as a little ductile fracture, so the failure of the knuckle can be attributed to brittle fracture distinctly.

In addition, a welding repair area with high hardness is found in the fracture region of the failed knuckle.

5.2. Based on the conclusions and analysis mentioned above, the fracture mechanism of the failed knuckle may be inferred as follows

The shrinkage porosity formed in the microstructure of the failed knuckle separated the metallic matrix and resulted in the reduction of plasticity, impact toughness and fracture resistance behavior of the knuckle, and improper welding repair might initiate micro-cracks on the surface of the knuckle. As a result, when the knuckle was subjected to an impact load that did not exceed knuckle material fracture limit during wagons running, the micro-cracks initiated from weld repair zone would propagated rapidly into the inner matrix by continuously fracturing the dendrites along shrinkage porosity regions, forming domino effect, until the knuckle failed instantly.

Acknowledgements

The authors would like to thank the Analysis and Test Center of Light Industry Department of Hubei University of Technology for their helping in this investigation work. Special thanks are given to Juan Song.

References

[1] American Association of Railroads: Manual of Standards and Recommended Practices Specification M 201 92 Steel Castings-Grade E, Rev; 1992.
[2] Chunduru SP, Kim MJ. Cliff Mirman failure analysis of railroad couplers of AAR type E engineering failure. Analysis 2011;18:374–85.
[3] Xiao L-m, Qin X-f. Fracture failure analysis of F51AE type coupler knuckles used in rio tinto group mineral freight cars. Journal of Dalian Jiaotong University 2011;4:43–7 [in Chinese].
[4] Infante V, Branco CM, Brito AS, Morgado TL. A failure analysis study of cast steel railway couplings used for coal transportation engineering failure. Analysis 2003;10(August (4)):475–89.
[5] Mousavi zadeh Noughabi SM, Dehghani K, Pouranvari M. Failure analysis of automatic coupler SA-3 in railway carriages engineering failure. Analysis 2007;14:903–12.
[6] Du Y-h, Zhang L, Xing S-m, Zhang P. Study on formation and mechanism of cracks in hook-head. Railway Locomotive and Car 2003;(3):21–3 [in Chinese].
[7] Boelena R, Curciob P, Cowinc A, Russell D. Ore-car coupler performance at BHP-Billiton iron ore engineering failure. Analysis 2004;11:221–34.
[8] Lu Y. Reasons for formation of fatigue cracks in domestic E class steel couplers and approach to eliminating cracks. Foundry 2008;(6):592–5 [in Chinese].
[9] Bai S-p. Analysis of formation causes and prevention measures of crack in 16, 17 type couplers for C 80 type wagons on Daqin railway line. Railway Quality Control 2008;(9):17–9 [in Chinese].
[10] Li X-h, Xie J-l. Prediction of Fatigue crack growth condition and life time on coupler guard arm area of E grade steel of burden strain. Journal of Beijing Jiaotong University 2006;(4):102–8 [in Chinese].
[11] Yu Z-w, Xu X-l, Mu X. Failure investigation on the cracked crawler pad link engineering failure. Analysis 2010;17:1102–9.